

1
2
3
4
5
6
7
8
9
10
11
12
13
14
15
16
17
18
19
20
21

**The Fluctuations of Blocked Ionic Current Reveal the
Instantaneous Statuses of DNA in Graphene Nanopore**

*Wenping Lv, Ren'an Wu**

CAS Key Lab of Separation Sciences for Analytical Chemistry, National Chromatographic R&A
Center, Dalian Institute of Chemical Physics, Chinese Academy of Sciences (CAS), Dalian,
116023, China

The corresponding Authors Footnotes:

Ren'an Wu (wurenan@dicp.ac.cn)
Tel: +86-411-84379828; Fax: +86-411-84379617

Wenping Lv (wenping@dicp.ac.cn)
Tel: +86-411-84379617; Fax: +86-411-84379617

22 **Abstract:**

23 Extracting the sequence information of DNA from the blocked ionic current is the
24 crucial step of the ionic current-based nanopore sequencing approaches. The thinnest
25 graphene nanopore, which contained only one layer of carbon atoms, potentially has
26 ultra-high DNA sequencing sensitivity. However, the dynamical translocation
27 information of DNA contained in the blocked ionic current has not been well
28 understood to date. In this letter, an assessment to the sensitivity of ionic
29 current-based graphene nanopore DNA sensing approach was carried out using
30 molecular dynamics simulations. By filtering the molecular thermal motion induced
31 noise of ionic current, we found that the instantaneous conformational variations of
32 DNA in graphene nanopore could be revealed from the fluctuations of the denoised
33 ionic current. However, the blockage of ionic current which induced by the proximity
34 of the DNA base-pairs to the nanopore (within 1.5 nm) was also observed. Although
35 the expected single-base resolution of graphene nanopore should be enhanced by
36 further studies, our findings indicated that the ionic current-based graphene nanopore
37 sensing approach has high sensitivity to the instantaneous translocation status of
38 DNA.

39

40

41

42

43

44

45

46 **Keywords:** graphene nanopore, molecular dynamics simulation, biosensors, DNA
47 sequencing, noise of ionic current, translocation status of DNA

48

49 Nanopore sequencing is a new technology promising to directly read out the gene
50 information of DNA at single-molecule level.^{1, 2} The center stage of nanopore
51 sequencing is to distinguish the signals of different kinds of bases of DNA through a
52 nanopore.³⁻⁹ The subnanometer thickness (0.34 nm) of graphene sheet comparable to
53 the spatial interval of DNA nucleotide suggests that the nanopore sequencing at
54 single-base level could be realized utilizing a graphene nanopore.^{4, 10} Based on
55 graphene nanopores created experimentally,¹¹ the translocation of double-stranded
56 DNA (dsDNA) through monolayer and/or multilayer graphene nanopores has been
57 recently demonstrated.⁵⁻⁷ In these experiments, the fluctuation of blocked ionic
58 current was observed, explained as the difference induced by folded/unfolded DNA or
59 the unzipping of DNA chains.⁵⁻⁷ Thanks to the atomic level molecular dynamics (MD)
60 simulation technology, the subtle structural features of DNA and the graphene-DNA
61 interactions during translocation could be further revealed. In 2011, Schulten et al.
62 observed the difference of ionic current blockages which induced by the
63 folded/unfolded DNA, and suggested that under suitable bias conditions A-T and G-C
64 base-pairs can be discriminated using graphene nanopores.¹² Recently, Aksimentiev et
65 al. reported that the translocation of single-stranded DNA (ssDNA) through graphene
66 nanopores might occur in single nucleotide steps,¹³ similar with the biologic
67 nanopores. However, the sensitivity of ionic current blockades to the orientations of
68 nucleotides in graphene nanopore has also been observed.^{13, 14}

69 Actually, ionic current-based nanopore sensing relies on ions through a nanopore
70 which contribute to both the signal and the noise.¹⁵⁻¹⁹ In particular, the membrane
71 capacitance produces noise fluctuations that increase with the bandwidths of
72 measurement,³ and the noise of ionic current in membrane-like graphene nanopore
73 was distinctly huger than that in the channel-like synthetic nanopore.^{12, 20} To reduce
74 the electrical noise of graphene nanopore, a stacked graphene-Al₂O₃ nanopore was
75 constructed and the temporal resolution of DNA and/or DNA-protein complexes
76 detection was significantly improved recently.²¹ Based on the differences of ionic
77 current, researchers found that the translocation of DNA in nanopores usually
78 accompanied with the deformation of DNA.^{12, 20, 22-24} Due to the atomic thickness of

79 graphene, the graphene nanopore sensors might have ultra-high sensitivity to the
80 instantaneous translocation statuses of DNA. However, the translocation information
81 of DNA contained in the fluctuation of blocked ionic current has not been well
82 understood to date.

83 Therefore, a systematic MD simulation study was presented in this letter, to explore
84 the sensitivity of ionic current to the instantaneous translocation statuses of DNA
85 within graphene nanopore. Before we extract the translocation information of DNA
86 from ionic current, the ionic current measurement itself ($I(t) = \{\sum_{i=1}^N q_i [z_i(t +$
87 $\Delta t) - z_i(t)]\} / \Delta t L z$) was assessed by investigating the fluctuation (root-mean-square,
88 RMS) dependencies of ionic current to the measure interval (Δt)^{16, 20}, simulation
89 temperature and bias voltage. By monitoring the variations of local conformation,
90 in-pore translocation velocity and graphene-DNA interaction of DNA within graphene
91 nanopore, how the conformational, dynamical and interactional information of in-pore
92 DNA revealed from the fluctuation of ionic current signal were presented. We found
93 that 1) the synchronous change of the number of atoms of DNA accumulated in
94 graphene nanopore and the blockage of ionic current was directly showed after the
95 thermal noise of ionic current has been filtered; 2) the blockage of ionic current could
96 also be induced by the proximity of DNA base-pairs to the nanopore. To the best of
97 our knowledge, it should be the first reported result dynamically shows the high
98 sensitivity of graphene nanopore to the instantaneous translocation statuses of in-pore
99 DNA.

100 As shown in Figure 1a, the interactions among ions, water molecules and graphene
101 directly impact the motion of the charge carriers (ions) in NaCl solution.²⁵ Therefore
102 the impact of measurement frequency ($1/\Delta t$) to the fluctuation of open-pore ionic
103 current was investigated with different temperatures (280K, 300K and 320K), bias
104 voltages (0V and 1V), graphene models (flexible and rigid) and cell dimensions (10
105 nm and 20 nm in z-direction). The obtained average (AVG) and fluctuation
106 (root-mean-square, RMS) of ionic currents were plotted as function of the measure
107 frequency ($1/\Delta t$) in Figure 1b-d. If no external bias voltage was applied (0V, 300K),
108 the average ionic current was maintained in zero because no directional movement of

109 ions was occurred in the system. While the fluctuation of ionic current was increased
110 with the rise of measure frequency linearly, indicating that the molecular thermal
111 motion (no bias voltage) induced Johnson-Nyquist (thermal) noise of ionic current
112 was sensitive to the choice of measure frequency. After the bias voltage (1V, 300K)
113 was applied, the fluctuation of the ionic current was even higher than the average
114 ionic current (8 nA) when Δt was shorter than 4 ps (250 GHz), and it was
115 undistinguishable with net thermal noise (0V, 300K). With the decrease of measure
116 frequency, the fluctuation of ionic current was reduced, but it still obviously greater
117 than net thermal noise, suggesting that the bias voltage could also induce the
118 enhancement of the noise of ionic current.¹⁵ Comparing the results of different
119 simulation temperatures (280K, 300K and 320K), the temperature sensitivity of both
120 average and fluctuation of ionic current were distinctly presented (Figure 1b),
121 suggesting that in a certain bias voltage the temperature determined molecular thermal
122 motion contributes significantly to the ionic current. Although the ions would also
123 accumulate on the surface of graphene nanopore for the oppression of applied electric
124 field,^{12, 25} but the impact of the shaking of carbon atoms at graphene nanopore edge
125 (Figure S2) to the fluctuation of ionic current (Figure 1c) was not as obvious as the
126 influence of temperature (Figure 1b). By the way, similar with the reported study for
127 biologic nanopore (α -Hemolysin),²⁶ the average ionic current could maintain steady
128 only if the time interval of measurements were shorter than 50 ps (> 20 GHz). The
129 abnormal drop of average ionic current might result from the periodic boundary
130 condition (PBC) employed in MD simulations, because it has been effectively
131 alleviated (Figure 1d) by using a bigger simulation cell (20 nm in z-direction). These
132 findings suggest that the “signal-to-noise” ratio could be improved by modulating the
133 measure frequency, analogous to the experimental and theoretical results that the
134 thermal noise of ionic current increases with the bandwidth of a detector.^{16, 18, 24-26}

135 Based on above discussions, the measure interval of ionic current in the following
136 studies was chose as 50 ps to ensure the “signal-to-noise” ratio > 5 (Figure 1d). The
137 microscopic kinetics of a dsDNA chain (d-poly(CAGT)₄₈) electrophoretically passing
138 through a 2.4 nm monolayer graphene nanopore were investigated based on 6 sections

139 of MD simulations (indexes 10-15 in Table S1). As shown in Figure 2a, the original
140 ionic current signals (grey lines) were further denoised with a FFT filter (cutoff
141 frequency was 10GHz) to remove the impact of the thermal noise (red lines).
142 Therefore, the presentation ability of ionic current to the instantaneous translocation
143 statues of DNA in graphene nanopore was improved (blue lines). The profiles of the
144 denoised ionic current (blue lines) were extremely different in the repeat MD
145 simulations (R1, R2 and R3), suggesting that the translation statuses of DNA in
146 graphene nanopore might be different in these simulations. To capture the
147 instantaneous dynamical information of DNA in graphene nanopore, the in-pore
148 translocation velocity of DNA was monitored:

$$149 \quad V(t) = \frac{1}{N(t)\Delta t} \sum_{i=1}^{N(t)} [z_i(t + \Delta t) - z_i(t)] \quad (1)$$

150 Namely, the in-pore velocity of DNA was defined as that within time interval of Δt the
151 displacement of the part of DNA located in graphene nanopore with a length of ΔZ ;
152 $N(t)$ represents the number of atoms of in-pore DNA at time point of t . The ΔZ was
153 chose as 1 nm in calculation. As shown in panels of [1V, R1], [1V, R2], [2V, R1] and
154 [2V, R2] in Figure 2b, although the bias voltage used in the calculations were 10 times
155 higher than that in experiments,^{1, 5, 6, 12} the translocation velocities of in-pore DNA
156 were fluctuated around 2 mm/ms (5.5 kbp/ms) and around 3 mm/ms (8.5 kbp/ms) in
157 most of the translocation time for 1 V and 2 V bias voltages, respectively. The
158 translocation velocities of DNA in these simulations seem to be comparable with that
159 of DNA which obtained experimentally using solid-state nanopores.²⁷⁻³⁰ While there
160 also were some unpredictable quick translocation events presented in these results,
161 suggesting that the translocations of DNA in graphene nanopore were unstable.
162 Especially, similar with the translocation of ssDNA in graphene nanopores,¹³ the
163 unceasing velocities fluctuations of DNA in simulations of [1V, R3] and [2V, R3]
164 showed that the translocation of dsDNA could also be stagnated in graphene nanopore.
165 The corresponding ionic current signals were fluctuated around 3 nA and 3.5 nA,
166 respectively. While for the other four results in Figure 2a, the magnitude of ionic
167 current signals were rose to the level of open-pore ionic current after about 12 ns ([1V,

168 R1]), 10 ns ([1V, R2]), 6 ns ([2V, R1]) and 5 ns ([2V, R2]), respectively. These results
169 indicated that not only the initial conformations of DNA (folded/unfolded), the
170 instantaneous translocation statuses of DNA could also impact the blocked ionic
171 current significantly.

172 Therefore, the undulates of the denoised ionic current (Figure 2a) were further
173 investigated to explore more detailed instantaneous translocation information of DNA.
174 As an example, the peaks and troughs of the denoised ionic current of [2V, R1] in
175 Figure 2a were marked with arrows a-g in Figure 3. Results show that the peaks and
176 troughs of blocked ionic current were corresponding to different local conformations
177 of DNA in graphene nanopore one by one (insets a-e of Figure 3). Meanwhile, the
178 trajectory of MD simulation (Movie S1) also dynamically shows that the
179 instantaneous conformational variations (such as yawing and upright) of in-pore DNA
180 did accompanied with the fluctuations of blocked ionic current. Different with the
181 stacking interaction-induced stepwise translocation of ssDNA in graphene nanopore,¹³
182 the instantaneous conformational variations induced velocity fluctuations of dsDNA
183 (Figure 2b) were more like a DNA deformation-induced translocation jam. The
184 comparison between the number of atoms of DNA accumulated in graphene nanopore,
185 $N(t)$, violet region of DNA in Figure 4a, and the ionic current signals (Figure 4b and
186 Figure S3) directly show that the fluctuations of blocked ionic current were reciprocal
187 to $N(t)$ elaborately for all the non-stagnant translocation events ([1V, R1], [1V, R2],
188 [2V, R1], [2V, R2]). However, a plane parameter “effective unoccupied area”, which
189 was proposed in a recent publication, could only basically reveal the spatial blockage
190 effect of DNA to the fluctuation of ionic current, because the spatial blockage effect
191 of DNA towards ionic current was reduced into a 2-dimensional (2D) parameter in
192 their model.³¹ These results indicate that not only the occupied area of nanopore, the
193 instantaneous conformational variations of the in-pore DNA was also a key factor of
194 the fluctuation of ionic current blockages.

195 The unstable translocations of DNA which revealed from the ionic current suggest
196 that the interactions between DNA and graphene were varied with the translocation.
197 As shown in Figure 4c, the DNA-graphene interaction was fluctuated in range of -25

198 ~ -150 kJ/mol in the first 3 ns. Compared with the average interaction energy (-27.08
199 \pm 6.32 kJ/mol) between a short in-pore DNA fragment composed of only two
200 base-pairs(ApT and GpC) and the same graphene nanopore (aperture 2.4 nm,
201 monolayer) in previous research,²⁴ the enhanced DNA-graphene interaction imply that
202 the nucleobases were exposed toward graphene surface (π - π stacking interaction was
203 much greater than edge-edge interaction between nucleobases and graphene^{32, 33}),
204 and/or the neighbor DNA base-pairs contributes to the DNA-graphene interaction also.
205 The MD trajectories (Movie S1-S2) showed that the exposed nucleobases did adhered
206 on the bottom of graphene nanopore steadily after 3 ns, according with the
207 dramatically enhancement of DNA-graphene interaction after 3 ns (inset of Figure 3c).
208 By the way, due to the strong π - π stacking interaction, the in-pore translocation
209 velocity of DNA was also reduced after 3ns, and the DNA translocation was almost
210 stagnated around 4 ns ([2V, R1] in Figure 2b). While, the energy barrier of the
211 bending of DNA and the strong electrostatic force applied on DNA which near to
212 graphene nanopore^{12, 24} induced the remaining DNA crosswise lying down and
213 blocked graphene nanopore closely (insets e-f of Figure 3 and Movies S1-S2). Thus
214 the adherence of DNA on graphene could also induce the unexpected fluctuations of
215 ionic current (marked with arrows e-f in Figure 3). After DNA passed through the
216 graphene nanopore (6~8 ns), the magnitude of ionic current (Figure 3) was rose to the
217 level of open-pore ionic current ($>$ 10 nA), and the structural fluctuation of graphene
218 nanopore (highlighted with yellow band in Figure 4d) was also decreased to the level
219 of no DNA system (Figure S2). Thus the fluctuations of the blocked ionic current
220 might also be influenced by the DNA-graphene interaction induced structural
221 fluctuations of graphene nanopore.

222 As we suggested above, the translocation statues of DNA base-pairs near to
223 graphene nanopore could also influence the fluctuation of ionic current. Thus a DNA
224 fragment composed of only two base-pairs (d-(AG)₂) was employed as a stopper to
225 probe the blockage effect of the neighbor base-pairs of DNA at pore entrance. A set of
226 MD simulations (indexes 16-59 in Table S1) were performed to get the ionic blockage
227 effect of the stopper at different positions and orientations. The shift range of the

228 stopper (probe DNA) to the center of graphene nanopore was $-2 \text{ nm} \sim 2 \text{ nm}$ (see insets
229 of Figure 5a). The schematic diagrams of the orientation altering of probe DNA were
230 shown as insets of Figure 5b. The obtained ionic blockages which induced by the
231 probe DNA with two orientations were shown in Figure 5a. We found that the blocked
232 ionic current (I) induced by DNA within graphene nanopore (distance was 0 nm) was
233 only about half of the open-pore current (I_o), it accords with the reported result.¹⁴ The
234 interesting result was that the DNA near to graphene nanopore could also induce the
235 ionic current blockages. For instance, when the probe DNA was positioned within 0.4
236 nm to graphene nanopore in z -direction, the blocked ionic currents were almost equal
237 to a half of the open-pore current (I_o), suggesting that the blockage effect of DNA
238 which near to the entrance of graphene nanopore towards ionic current (I/I_o) was
239 similar to that of DNA within nanopore (Figure 5b). Additionally, the ionic current
240 blockages were enhanced with the decrease of the DNA-graphene interval (Figure 5a)
241 when the probe DNA was positioned within 1.5 nm of graphene nanopore. The
242 neighborhood effect of DNA to ionic current blockage indicated that the
243 conformational variation of the neighbor base-pairs of DNA around graphene
244 nanopore entrance could also induce the fluctuation of ionic current.

245 In summary, a series of MD simulations were carried out to assess the ionic current
246 measurement and to extract the instantaneous translocation information of DNA in
247 graphene nanopore from the fluctuations of blocked ionic current. A key result of our
248 study was that the instantaneous conformational variations of in-pore DNA were
249 synchronously revealed from the undulations of denoised ionic current because the
250 fluctuation of the number of atoms of DNA accumulated in graphene nanopore.
251 However, we also found that both the DNA base-pairs within and near to the entrance
252 of graphene nanopore have similar blockage effect to ionic current. Compared with
253 other sensing approaches based on graphene (*i.e.* the transverse conductance
254 measurement of graphene nanopore,³⁴ nanoelectrode³⁵ and nanoribbon³⁶ etc.), the
255 DNA base-specific resolution of the ionic current-based graphene nanopore sensing
256 should be further improved. Modifying the graphene nanopore with functionalized
257 groups,³⁵ might be a potential strategy to enhance the DNA base distinguish ability of

258 ionic current based on graphene nanopore sequencing system.

259

260

261 **Acknowledgement:**

262 This work was supported by the National Natural Science Foundation of China (No.
263 21175134), the Knowledge Innovation Program of Dalian Institute of Chemical
264 Physics and the Hundred Talent Program of the Chinese Academy of Sciences to Dr.
265 R. Wu.

266

267 **Supporting information Available:**

268 Detailed description of the simulation methods; plot of the average and fluctuation
269 of the ionic current obtained from the three benchmark MD simulations by using
270 different temperature coupling methods (nose-hoover, berendsen and v-rescale); plot
271 of the root-mean-square distances (RMSD) of the flexible and rigid graphene
272 nanopores; plots of the comparing of ionic current and number of DNA atoms in
273 graphene nanopore for the simulation [1V, R1], [1V, R2], [1V, R3], [2V, R2] and [2V,
274 R3]; list of the detail simulation parameters of all the calculations in our work;
275 animations illustrating of the synchronically evolution of the MD trajectory of
276 d-poly(CAGT)₄₈ DNA translocation in graphene nanopore and the fluctuation of
277 blocked ionic current as well as the molecular details of DNA adhering on graphene
278 surface.

279

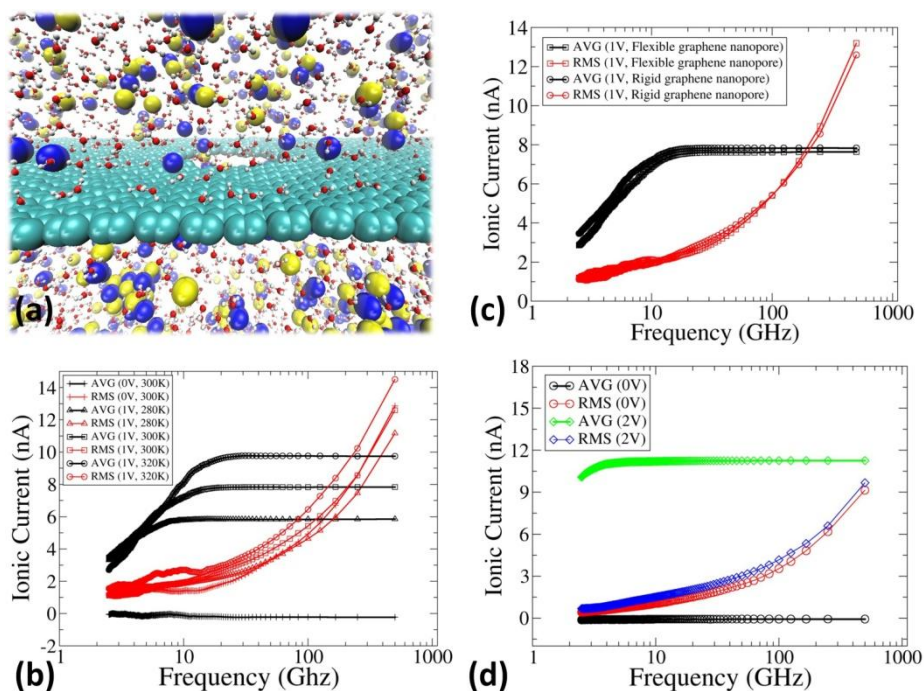
280 **Reference:**

- 281 1. B. M. Venkatesan and R. Bashir, *Nat Nanotechnol*, 2011, **6**, 615-624.
- 282 2. H. Kumar, Y. Lansac, M. A. Glaser and P. K. Maiti, *Soft Matter*, 2011, **7**, 5898-5907.
- 283 3. M. Wanunu, *Physics of life reviews*, 2012, **9**, 125-158.
- 284 4. Z. S. Siwy and M. Davenport, *Nat Nanotechnol*, 2010, **5**, 697-698.
- 285 5. G. F. Schneider, S. W. Kowalczyk, V. E. Calado, G. Pandraud, H. W. Zandbergen, L. M. K.
- 286 Vandersypen and C. Dekker, *Nano Lett*, 2010, **10**, 3163-3167.
- 287 6. C. A. Merchant, K. Healy, M. Wanunu, V. Ray, N. Peterman, J. Bartel, M. D. Fischbein, K. Venta,
- 288 Z. T. Luo, A. T. C. Johnson and M. Drndic, *Nano Lett*, 2010, **10**, 2915-2921.
- 289 7. S. Garaj, W. Hubbard, A. Reina, J. Kong, D. Branton and J. A. Golovchenko, *Nature*, 2010, **467**,
- 290 190-U173.
- 291 8. D. Branton, D. W. Deamer, A. Marziali, H. Bayley, S. A. Benner, T. Butler, M. Di Ventra, S. Garaj,
- 292 A. Hibbs, X. H. Huang, S. B. Jovanovich, P. S. Krstic, S. Lindsay, X. S. S. Ling, C. H. Mastrangelo,
- 293 A. Meller, J. S. Oliver, Y. V. Pershin, J. M. Ramsey, R. Riehn, G. V. Soni, V. Tabard-Cossa, M.
- 294 Wanunu, M. Wiggin and J. A. Schloss, *Nat Biotechnol*, 2008, **26**, 1146-1153.
- 295 9. C. Dekker, *Nat Nanotechnol*, 2007, **2**, 209-215.
- 296 10. M. S. Xu, D. Fujita and N. Hanagata, *Small*, 2009, **5**, 2638-2649.
- 297 11. M. D. Fischbein and M. Drndic, *Appl Phys Lett*, 2008, **93**.
- 298 12. C. Sathe, X. Q. Zou, J. P. Leburton and K. Schulten, *Acs Nano*, 2011, **5**, 8842-8851.
- 299 13. D. B. Wells, M. Belkin, J. Comer and A. Aksimentiev, *Nano Lett*, 2012, **12**, 4117-4123.
- 300 14. J. Comer and A. Aksimentiev, *J Phys Chem C*, 2012, **116**, 3376-3393.
- 301 15. W. Z. Qiu, T. C. Nguyen and E. Skafidas, *Ieee Sens J*, 2013, **13**, 1216-1222.
- 302 16. A. Aksimentiev, *Nanoscale*, 2010, **2**, 468-483.
- 303 17. R. M. M. Smeets, N. H. Dekker and C. Dekker, *Nanotechnology*, 2009, **20**.
- 304 18. V. Tabard-Cossa, D. Trivedi, M. Wiggin, N. N. Jetha and A. Marziali, *Nanotechnology*, 2007, **18**.
- 305 19. R. M. M. Smeets, U. F. Keyser, N. H. Dekker and C. Dekker, *P Natl Acad Sci USA*, 2008, **105**,
- 306 417-421.
- 307 20. A. Aksimentiev, J. B. Heng, G. Timp and K. Schulten, *Biophys J*, 2004, **87**, 2086-2097.
- 308 21. B. M. Venkatesan, D. Estrada, S. Banerjee, X. Z. Jin, V. E. Dorgan, M. H. Bae, N. R. Aluru, E. Pop
- 309 and R. Bashir, *Acs Nano*, 2012, **6**, 441-450.
- 310 22. A. F. Sauer-Budge, J. A. Nyamwanda, D. K. Lubensky and D. Branton, *Phys Rev Lett*, 2003, **90**.
- 311 23. B. Lu, F. Albertorio, D. P. Hoogerheide and J. A. Golovchenko, *Biophys J*, 2011, **101**, 70-79.
- 312 24. W. Lv, M. Chen and R. a. Wu, *Soft Matter*, 2013, **9**, 960-966.
- 313 25. G. H. Hu, M. Mao and S. Ghosal, *Nanotechnology*, 2012, **23**.
- 314 26. A. Aksimentiev and K. Schulten, *Biophys J*, 2005, **88**, 3745-3761.
- 315 27. A. J. Storm, J. H. Chen, H. W. Zandbergen and C. Dekker, *Phys Rev E*, 2005, **71**.
- 316 28. B. M. Venkatesan, A. B. Shah, J. M. Zuo and R. Bashir, *Adv Funct Mater*, 2010, **20**, 1266-1275.
- 317 29. B. M. Venkatesan, B. Dorvel, S. Yemenicioglu, N. Watkins, I. Petrov and R. Bashir, *Adv Mater*,
- 318 2009, **21**, 2771-+.
- 319 30. A. J. Storm, C. Storm, J. H. Chen, H. Zandbergen, J. F. Joanny and C. Dekker, *Nano Lett*, 2005, **5**,
- 320 1193-1197.
- 321 31. L. J. Liang, P. Cui, Q. Wang, T. Wu, H. Agren and Y. Q. Tu, *Rsc Adv*, 2013, **3**, 2445-2453.
- 322 32. R. R. Johnson, A. T. C. Johnson and M. L. Klein, *Small*, 2010, **6**, 31-34.

- 323 33. W. P. Lv, *Chem Phys Lett*, 2011, **514**, 311-316.
- 324 34. K. K. Saha, M. Drndic and B. K. Nikolic, *Nano Lett*, 2012, **12**, 50-55.
- 325 35. Y. H. He, R. H. Scheicher, A. Grigoriev, R. Ahuja, S. B. Long, Z. L. Huo and M. Liu, *Adv Funct*
326 *Mater*, 2011, **21**, 2674-2679.
- 327 36. S. K. Min, W. Y. Kim, Y. Cho and K. S. Kim, *Nat Nano*, 2011, **6**, 162-165.
- 328
- 329
- 330
- 331

332 **Figures and Legends:**

333

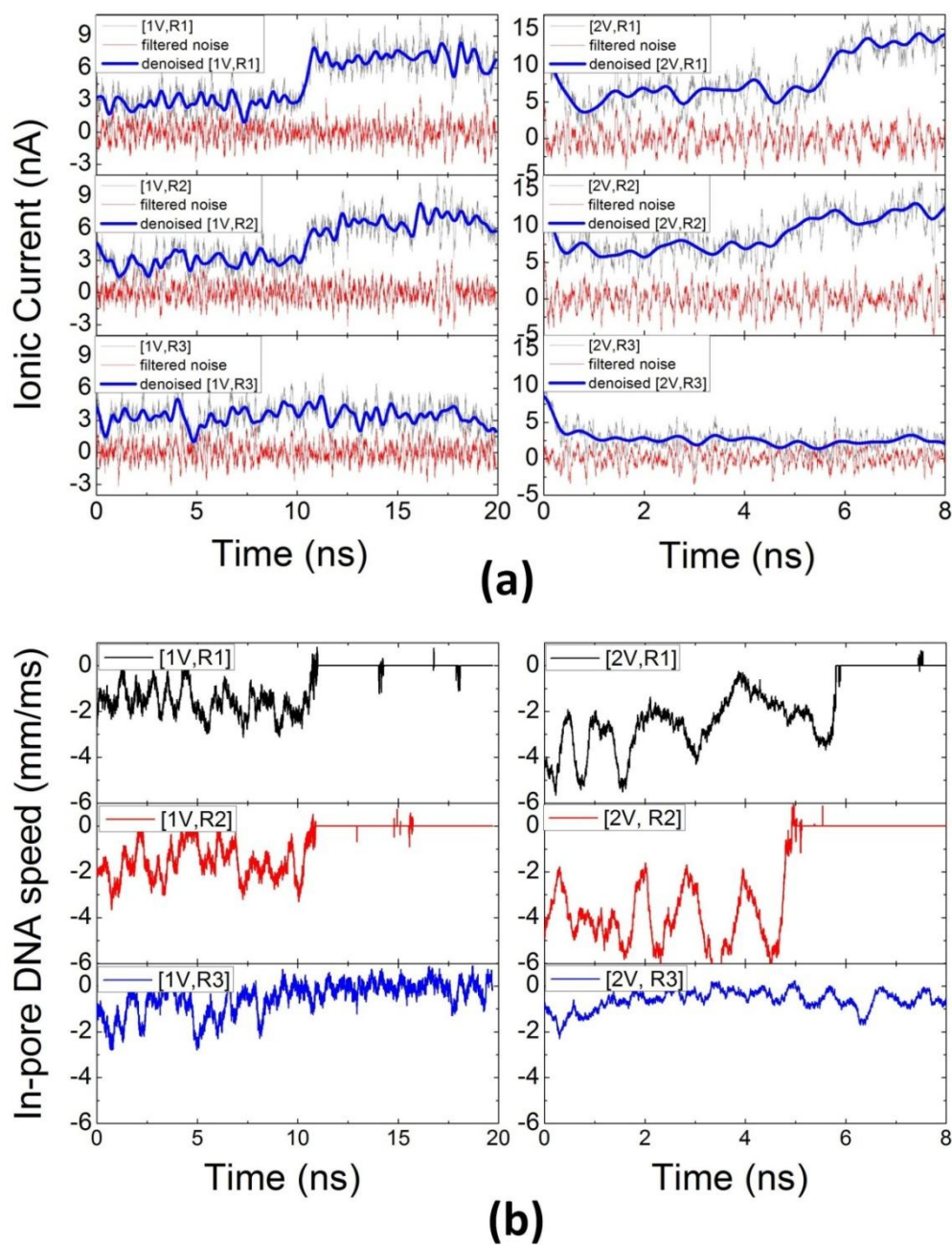


334

335 Figure 1. (a) The schematic diagram of open-pore ionic current simulation. The Na⁺,
 336 Cl⁻ and graphene nanopore were colored with yellow, blue and cyan in “VDW
 337 model”. For representation convenience, here only 10% of the water molecules in
 338 simulation system were showed in “CPK model”. (b-d) The average (AVG) and the
 339 fluctuation (root-mean-square, RMS) of open-pore ionic current for the simulations
 340 of (b) different temperature and bias voltage, of (c) flexible and rigid graphene
 341 nanopores and of (d) the big simulation box (6.3x6.3x20 nm³) were plotted as
 342 function of the measure frequency (1/ Δt). Data were obtained from the last 3-ns of
 343 the 4-ns MD trajectories.

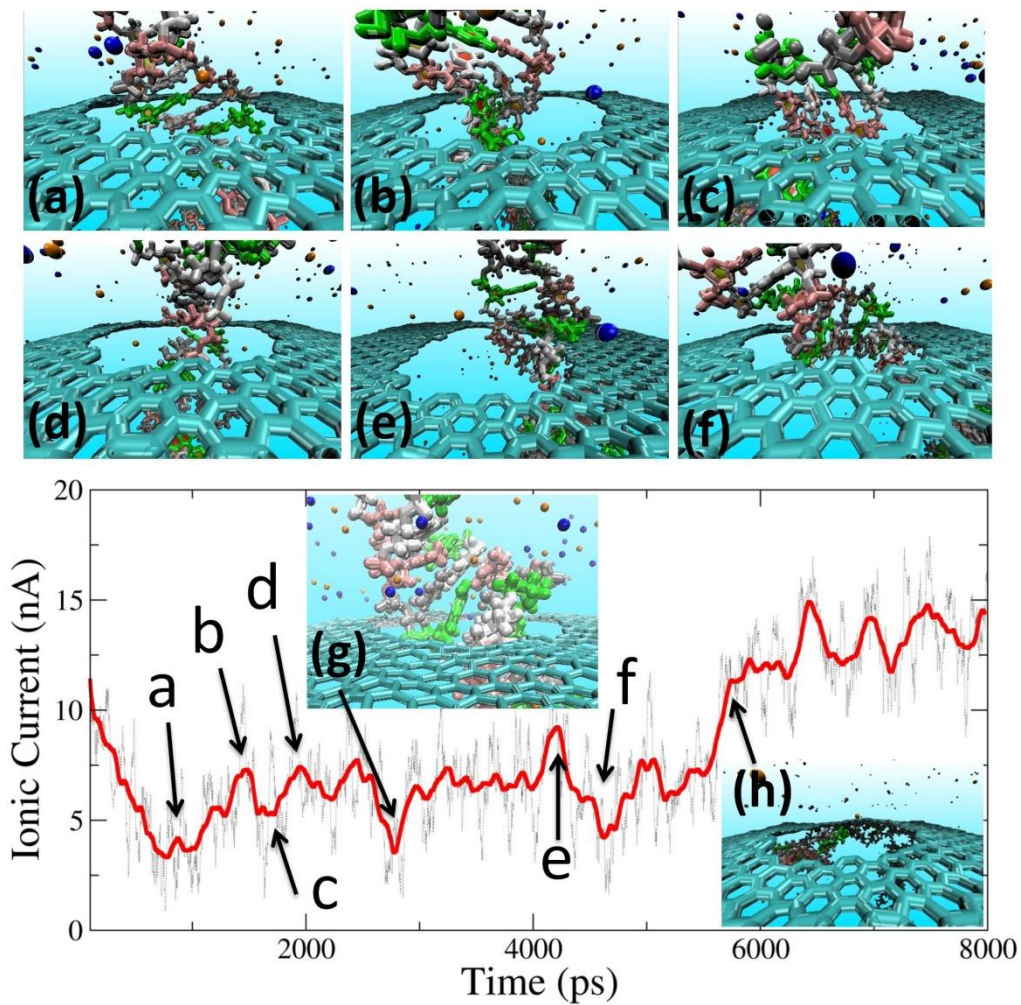
344

345

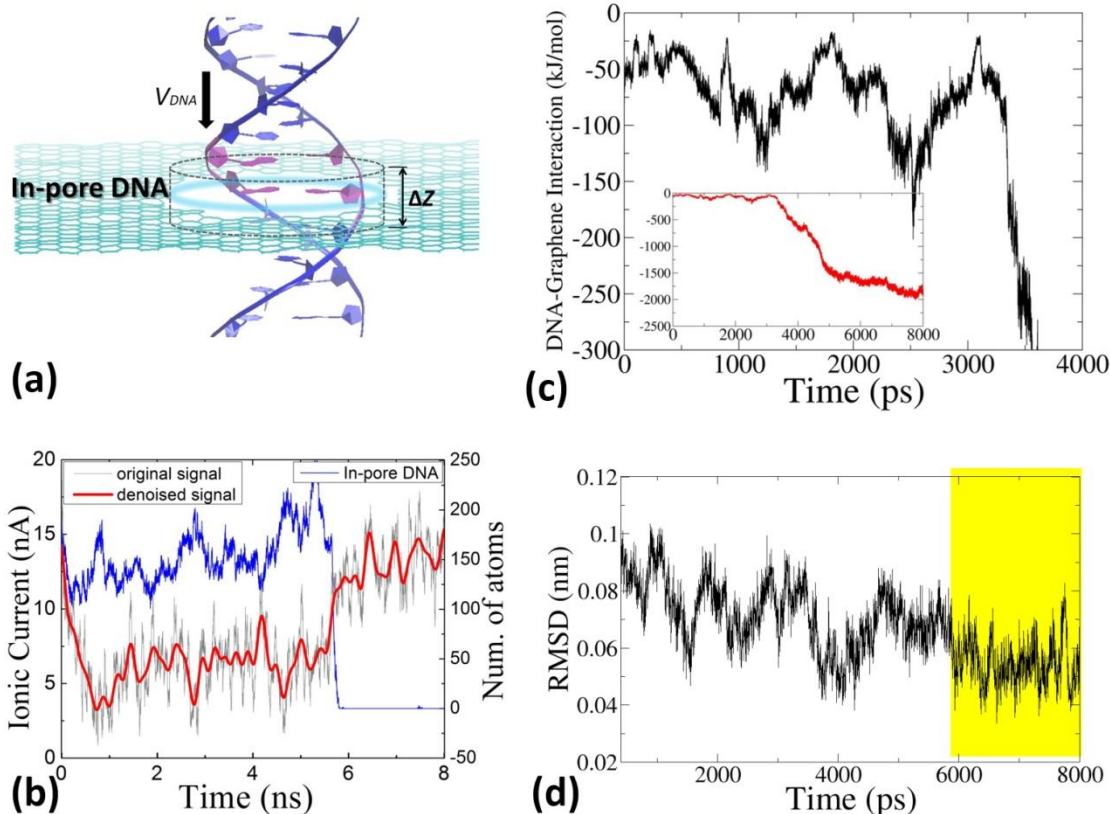


346

347 Figure 2. (a) The ionic current signals (grey lines) which obtained from the MD
 348 simulations of 10-15 in Table S1 were plotted as function of simulation time. The
 349 denoised ionic current signals (blue lines) were smoothed by a FFT filter with cutoff
 350 frequency of 10GHz. The filtered noises were also presented (red lines). (b) The
 351 instantaneous translocation velocity of DNA in graphene nanopore was plotted as
 352 function of simulation time. In all the legends, the 1V and 2V were the applied bias
 353 voltages; the R1, R2 and R3 were used to label the three repeated MD simulations.



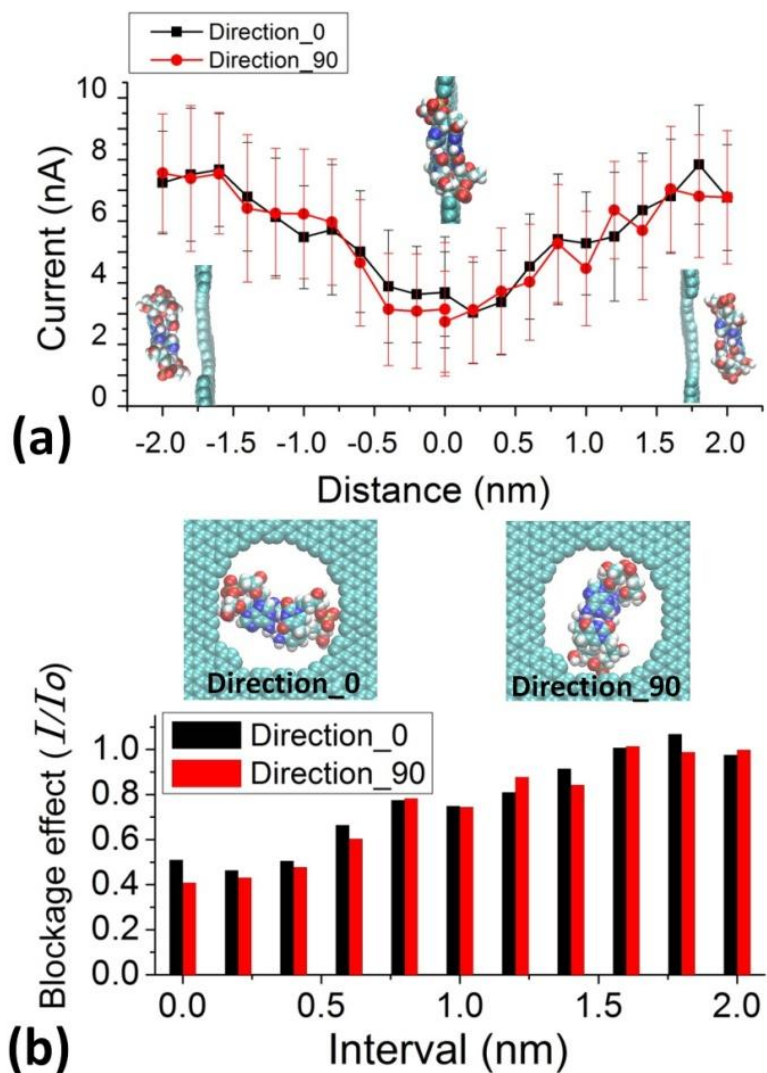
354
 355 Figure 3. Both of the original (grey line) and smoothed (red line) ionic current were
 356 plotted as function of simulation time. The insets (a-h) show the local conformations
 357 of DNA in graphene nanopore, which is corresponding to the undulate of ionic current
 358 (marked with arrows a-h).



359
360

361 Figure 4. (a) The representation of in-pore DNA (colored in violet), ΔZ was set to 1
362 nm. (b) The time evolutions of the accumulated number of atoms of DNA
363 accumulated in graphene nanopore (blue line) and ionic current signals (red line and
364 grey line) of the simulation [2V, R1]. (c) The time evolution (0-4 ns) of the interaction
365 energy between DNA and graphene of simulation [2V, R1]. The DNA-graphene
366 interaction energy of whole trajectory was also showed as inset (0-8ns). (d) The time
367 evolution of the root-mean-square distance (RMSD) of graphene nanopore of
368 simulation [2V, R1]. The yellow band highlighted that the magnitude of RMSD of
369 graphene nanopore was reduced after the translocation of DNA has finished (about
370 6-8ns).

371



372

373 Figure 5. (a) The ionic current was plotted as function of the separation between DNA
 374 fragment and graphene nanopore. (b) The blockage effect of DNA to ionic current
 375 (I/I_o) with two orientations was plotted as function of interval between DNA and
 376 graphene nanopore. I_o is the open pore ionic current of the graphene nanopore. The
 377 schematic diagrams of the position and orientation altering of DNA fragment in ionic
 378 current calculations were shown as insets.

379